Carrier Plane Design for the AIAA DBF Competition

Kota Mitsumoto[1], Ryan Maye[2], Duncan Green[3]
The University of Alabama in Huntsville, Huntsville, Alabama, 35805, USA

SPAROW is a student-led engineering team aiming to compete in AIAA's 2025 Design/Build/Fly competition. The challenge involves two airframes, an autonomous glider and a mothership for deploying the glider mid-flight. This paper covers the research, design process, and reasoning that led to the mothership's final airframe design. A sensitivity analysis of the competition scoring system was initially conducted to identify the flight performance parameters that would maximize the overall score. Based on these findings, our design philosophy prioritized weight and drag reduction to achieve a high cruise speed. We then carried out trade studies on various airframe configurations, exploring alternatives beyond conventional glider geometry. Concepts such as flying wings, multiple fuselages, A-tail, and V-tail designs were considered to stabilize the unsteady two-body interactions caused by turbulent flow during the mid-flight separation of the glider. For carrying and deploying the glider, pitch stability proved to be a critical factor that disqualified designs that lacked a rear stabilizer. Additionally, we implemented a retractable landing gear mechanism to provide the necessary ground clearance for housing the glider. Detailed geometric dimensions were derived based on expected flight performance and mass distribution. Lastly, CAD modeling and XFLR5 simulations were conducted to validate component integration and assess flight stability. We successfully developed an airframe design that met the desired flight performance objectives, supported by thorough analysis and research. Additionally, its feasibility was confirmed through simulations, ensuring a smooth transition to the manufacturing phase of the program while minimizing the costs associated with experimental prototyping.

Nomenclature

Re = Reynold's number

ρ = Air density

v = velocity

b = Wingspan

c = Chord

S = Wing area

AR = Aspect ratio

Cl = Lift coefficient

Cd = Drag coefficient

Cm = Moment coefficient

AoA = Angle of attack

CG = Center of gravity

[1] Undergraduate, Mechanical and Aerospace Engineering Dept, km0257@uah.edu, Student Member, 1760261
[2] Undergraduate, Mechanical and Aerospace Engineering Dept, rkm0016@uah.edu, Student Member, 1605403
[3] Undergraduate, Mechanical and Aerospace Engineering Dept, drg0020@uah.edu, Student Member, 1605211

I.   Introduction

SPAROW (Subsonic Plane Autonomized with Reliable Optimized Wings) is a student team within the University of Alabama's Space Hardware Club. The team aims to compete in the American Institute of Aeronautics and Astronautics's (AIAA) annual Design Build Fly (DBF) competition. The 2025 DBF competition required the team to produce two fixed-wing Unmanned Aerial Vehicles (UAVs), the carrier and the glider. The carrier is the mothership that takes off carrying the glider and deploys the glider mid-flight. After the separation, the glider flies autonomously to a predetermined ground coordinate. The carrier is also required to perform certain missions, such as lap flights around a course with and without a payload. This paper covers the research and development of the carrier plane. A sensitivity analysis on the competition scoring system was conducted to find the dependent parameters that affect the total points. Latter development was based on design principles established based on the sensitivity analysis results. The design of the carrier airframe was determined in parallel to computational simulations, ensuring the design would have the desired flight characteristics, such as stability and cruise velocity. Lastly, CAD was used for weight management and to finalize the carrier design.

Recently, the use of UAVs has become widespread over various fields, from agriculture to military sectors [1,2]. Commercial drone services are revolutionizing fields such as surveillance and transportation. For instance, ZIPLINE established a network of fixed-wing drones over the skies of Rwanda for medical supply transportation [3]. The unique characteristics of fixed-wing drones, having high cruising velocity, range, and cost efficiency, have a large potential and are expected to expand use over the years. Thus, the objective of SPAROW is not only to compete in the DBF competition. Knowledge and experience gained through research and development of the fixed-wing drone will have a huge impact on each team member's engineering perspective and career as we enter a field more and more filled with UAVs. Providing such learning opportunities is the primary objective of the SPAROW program.

II.   Sensitivity analysis

The AIAA DBF competition has multiple challenges, and scores are applied accordingly to the performance of each challenge element. The final result of the competition will be the sum of the scores; thus, finding the effectiveness factor of the score elements to the total score was crucial for aiming for high points. The key challenge elements were simulated fuel weight, flight lap time, number of laps, glider weight, and ground mission time. Simulated fuel is a pod-detachable load that simulates an external fuel tank. The ground mission requires quick operation of attaching fuel loads and their pylons to the carrier. Figure 1 shows the result of the sensitivity analysis, showing the percent change in the total score induced by the percent change in each challenge element performance. The effectiveness is proportional to the slope of the plot lines. Based on the results and design limitations from DBF requirements, internal team design requirements were created, as shown in Table 1. As the plot indicated, the high cruise speed of the carrier resulting in better lap time had the most impact on the total score. As a result, the carrier's main design principle was determined to focus on the reduction of aerodynamic drag and airframe weight for maximum efficiency at high cruise velocity.
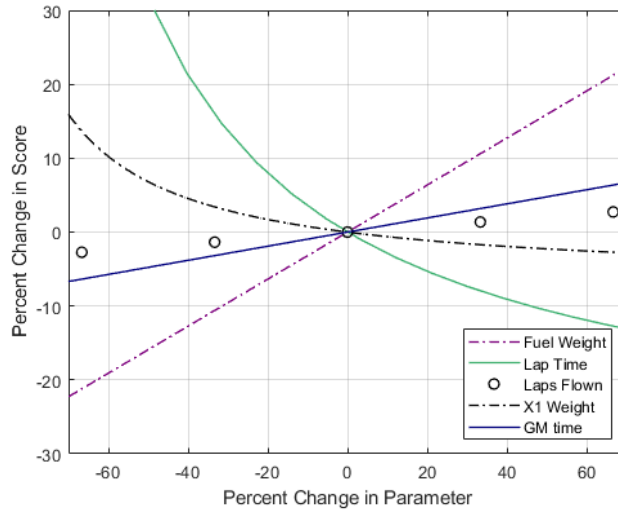
Figure 1 Sensitivity of score by input parameter variation

Req. #	Description
1	Carrier shall not weigh more than 55 pounds
2	Carrier shall not have a wingspan in excess of 6 feet
3	Carrier shall be able to carry the test vehicle
4	Carrier shall be able to release the test vehicle
5	Carrier shall be able to mount 2 simulated external fuel tanks
6	Carrier shall be capable of having fuel tank pylons removed
7	Carrier shall be capable of ground takeoff
8	Carrier shall be capable of ground landing
9	The total stored propulsion power must not exceed 100 Watt-Hours
10	The Carrier must be controlled by manual flight performed by a pilot
11	The Carrier must not be controlled with flight controllers

Table 1 AIAA DBF Requirements for Carrier Plane

III. Conceptual Design and Analysis

As mentioned in the previous section, the sensitivity analysis revealed that the total competition point strongly correlates with the carrier's cruise velocity. Thus, the main design principle of the carrier was achieving a high cruising velocity by reducing aerodynamic drag and weight.

As the starting point of the carrier design, the DBF requirements roughly predetermined the total weight and size of the glider. To achieve a high cruising speed, two 500kv brushless motors powered by two 2200mAh 6s LiPo batteries were selected to provide 9 minutes of flight time. In addition, the competition required the carrier to carry a simulated fuel load, for which we planned to take 40 oz of payload. The airframe was planned to be constructed from carbon fiber tubes covered with a fiberglass shell. The main wing will be constructed from a

fiberglass-reinforced foam core. These materials were selected due to their low density, cost-effectiveness, and reparability. In total, the carrier was estimated to weigh 8-10 lbs. Due to the maximum wingspan limit of 6 ft as set by the DBF requirements, various wing chords were considered to achieve an adequate wing loading for the carrier. The optimal wing design was determined to be a tip-tapered geometry with the main chord length of 10 in, which resulted in the wing area of 687 in^2, aspect ratio of 7.5, and wing load of approximately 0.013 lb/in^2. From the rating of the brushless motors, the target cruise velocity was set to 67.5 mph (30 m/s), and the target minimum velocity to 22.5 mph (10 m/s) to minimize the airstrip required to take off and land. The Reynolds number of the wing based on chord length was calculated at cruise and minimum velocities to serve as a reference for aerodynamic simulations. At cruise, the Re was 5x10^5 and at minimum velocity was 1.4x10^5.

$$Re = \frac{\rho v c}{\mu} \tag{1}$$

Re_cruise (67.5 mph)	5x10^5
Re_minimum (22.5 mph)	1.4x10^5

Table 2 Reynolds number at cruise and minimum velocity

Based on the determined glider dimensions, three airframe types were considered: flying wing, single fuselage, and double fuselage, as shown in Figure 2. Flying wing is a common configuration for UAVs due to its aerodynamic efficiency and relative ease of manufacturing. Single fuselage is the most common airframe structure. Double fuselage has a wide open space under the center of the wing, which is optimal for housing the glider. From an aerodynamics efficiency standpoint, the flying wing had an advantage over the other two since the whole fuselage could be used to generate lift. However, the pitch stability of a flying wing design is extremely sensitive to the position shift of the CG. Since the design does not have a tail, the passive aerodynamic stability is fully determined by the positioning of the wing's center of lift and CG. Thus, compared to types having a tail, shifting the flying wing's CG has a larger influence on the pitch stability. Considering the carrier must deploy the glider mid-flight, both the center of pressure and CG are expected to shift during flight. Since we could not prove that the shifts were inconsequential to the stability of the flying wing design, we did not choose the flying wing type design.

From an aerodynamic point of view, the single-fuselage and double-fuselage types are similar. However, the double-fuselage is superior as it can house the glider under the wing, while the single-fuselage type forces the glider to be stored under the main fuselage. To create space for the glider on the single-fuselage configuration, the landing gear would need to be long and require a low-wing design to create enough ground clearance. This may overcomplicate the landing gear and nacelle design, thus increasing weight. Furthermore, the low-wing configuration may lack roll stability and thus require adding a dihedral angle to the wing or more roll adjustment from the pilot input. On the contrary, as mentioned before, the double-fuselage type has a large clearance under the wing for glider housing. Furthermore, since the center fuselage does not exist, the wing can be shifted upwards into a high-wing configuration. The two fuselage and nacelle structures can be mounted under the wing, resulting in shorter landing gear. Given the advantages, the double-fuselage design was optimal as it met the requirement to deploy a glider mid-flight while being as light as possible.

The one problem it had was the possibility of the glider colliding with the tail due to an unstable updraft. This concern was solved by adopting an A-tail design. The A-tail replaced the horizontal and vertical stabilizer with an inverted V-tail-like structure, leaving the space between the two fuselage tails for the glider separation. The slight instability induced by the anhedral angle of the A-tail was considered to be minimal and could be compensated for with pilot input. In addition, applying dihedral to the main wing was proposed; however, considering our limitation on manufacturing precision, there was a risk of creating a wing with asymmetrical dihedral. Since the plane will fly at a high velocity, even a small unbalance might prove critical during flight. Thus, it was decided that applying a dihedral angle was not practical for this year's design, however, it will be reconsidered for future projects once we gain new high-precision manufacturing techniques for the wing. For the current project, the experience of the pilot covers the slight roll instability of the carrier.
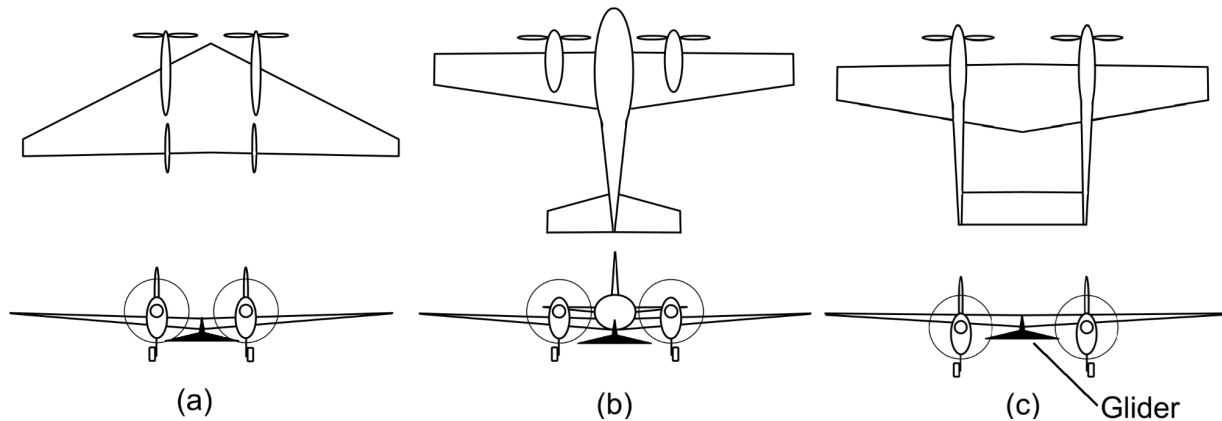
Figure 2 Conceptual draft of three airframe types: (a) Flying wing (b) Single fuselage (c) Double fuselage

Based on the results of the carrier conceptual design discussion, other carrier design parameters were determined. These parameters were tested computationally using XFLR5 simulation software. XFLR5 is a tool for analyzing the basic aerodynamic performance of fixed-wing RC planes. Since the carrier is in the Reynolds number regime similar to that of RC planes, XFLR5 was a useful workbench for testing the ideas without producing a prototype. This helped the project to develop rapidly with minimum cost spent on the research and development stage. All simulations were conducted at Re = 5x10^5.

Initially, a 2D airfoil analysis was conducted to find the optimum airfoil for the carrier. Four types of airfoils were selected for comparison: NACA0012, NACA2412, ClarkY, and SD7037. NACA0012 and NACA2412 were the most generic symmetric and non-symmetric airfoils. ClarkY is an airfoil often used in small-sized planes and RC planes. SD7037 is an airfoil commonly used in RC performance gliders. Each profile of the airfoil is shown in Figure 3 below. Cl and Cl/Cd values were calculated as shown in plots (a) and (b) in Figure 4. Results indicated that the ClarkY airfoil best matched the requirements of the carrier. From the Cl/Cd plot, both ClarkY and SD7037 had over 50% larger value than the asymmetric NACA2412 airfoil, indicating both could achieve a high glide slope ratio at small AoA conditions. Furthermore, the peak positions of each plot indicated that the peak efficiency of ClarkY and SD7037 airfoils were at AoA=4 degrees compared to that of NACA0012 and NACA2412 at AoA=6 degrees. The difference between ClarkY and SD7037 could be seen from the Cl plot stall characteristics. ClarkY had a higher stall angle at AoA=12 degrees compared to AoA=11 degrees of SD7037. In addition, the decrease of Cl due to stall is more moderate with ClarkY. Such stall characteristics are necessary for the carrier as it will be remotely controlled from the ground, which means that the pilot receives minimal feedback about the stall margins. The ClarkY airfoil was concluded to perform best for the carrier due to its low-drag, high-lift, and moderate stall profile. For the tail, NACA0012 was used as it is a symmetric airfoil with enough thickness to maintain the strength and contain the electrical wiring inside.
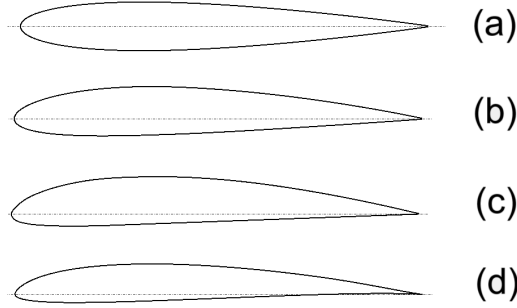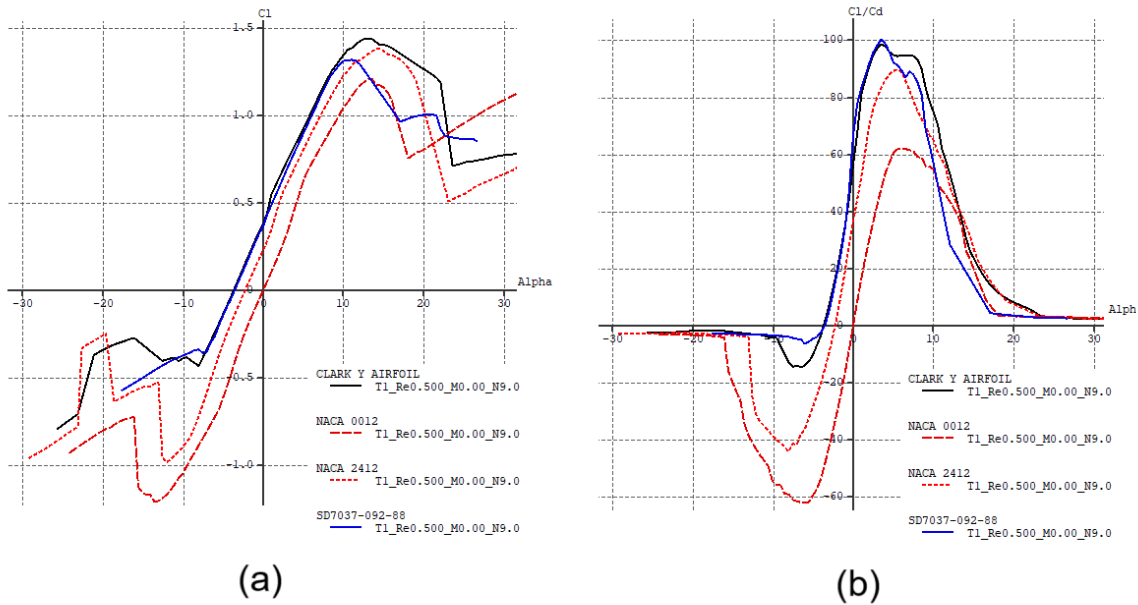
Figure 3 Profiles of tested airfoils: (a) NACA0012 (b) NACA2412 (c) ClarkY (d) SD7037

Figures 4 2D Airfoil analysis results: (a) Cl vs AoA (b) Cl/Cd vs AoA

The carrier model was simulated in XFLR5 to estimate the cruise flight velocity and pitch stability. Due to computation limitations, only the wing and tail were simulated, ignoring the fuselage and propeller downwash effects. Thus, this simulation was intended to be an early indicator of the carrier design performance and not a complete real-world flight characteristic simulation. For further detailed flight characteristics analysis, experimental flight tests with the prototypes will be conducted. In parallel with the simulation, fine carrier parameters such as the main wing-induced angle, CG position, and tail area were determined. Figure 6 (a) shows the simulated model's visual representation.

Figure 5 (a) shows the velocity needed to maintain a level flight at given AoA with various main wing induced angles. We have decided to give a negative induced angle to the main wing attachment since the initial case had a cruise velocity of 36 mph (16 m/s), significantly lower than the target cruise velocity of 67.5 mph. This was due to the excess lift generated by the efficient ClarkY airfoil, resulting in less velocity to maintain a level flight.

This characteristic would be optimum for soaring gliders; however, for a high-speed plane, a negative induced angle was preferable to decrease the amount of lift generated. A negative included angle of 1.5 degrees gave approximately 67.5 mph at AoA=0, as shown in the plot. Furthermore, Figure 5 (b) indicates the pitch stability tolerance to CG shift. The CG was varied from 20-30% chord length from the leading edge to simulate nose-heavy and tail-heavy conditions. These simulations were necessary since the deployment of the glider and the simulated fuel load may shift the CG of the carrier. The Cm had a negative relationship, indicating passive pitch stability, and the moments created at AoA=0 due to CG shift were minimum. These data confirmed that the prototype based on current parameters would likely have a passive stability optimum for further flight tests.

The wing-induced negative angle also increased the minimum velocity of the carrier; thus, flaps had to be introduced. Since the outer wing trailing edge had ailerons and the center section between the fuselages was being used to mount the glider, the ideal position of the flaps was determined to be between the fuselage and the inner edge of the aileron. The simulated model of the carrier with flaps deployed is shown below in Figure 6 (b). 25% of the chord was allocated to the flap section. From the simulation result shown in Figure 5 (c), the velocity reduced to 20.25 mph (9 m/s) with the flap deployed, which is below the targeted 22.5 mph minimum velocity. Figure 5 (d) proves that the lift was increased drastically due to flap deployment, however, drag is also increased. Thus, the use of flaps must be reserved for takeoff and landing as our main goal is to score high points from high cruising speed.

As a result of the consideration of multiple designs and verification using XFLR5 simulations, the aerodynamic design was defined, which allowed for work to begin on the CAD model of the aircraft and the eventual manufacturing of a prototype aircraft. The final design geometry is shown in Figure 7.
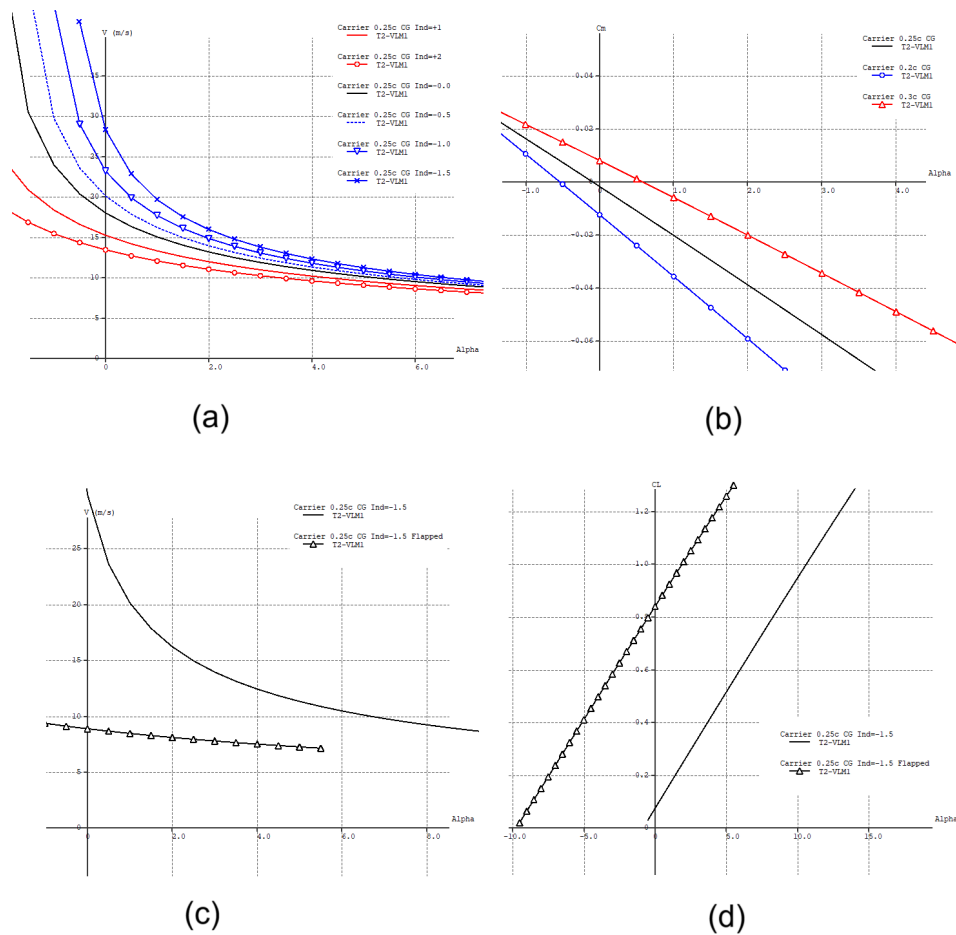

(a)

(b)

(c)

(d)

Figure 5 Carrier model analysis results: (a) Cruise velocity vs AoA with various wing induced angle (b) Cm vs AoA with various CG shift (c) Cruise velocity vs AoA with Flap (d) CL vs AoA with Flap
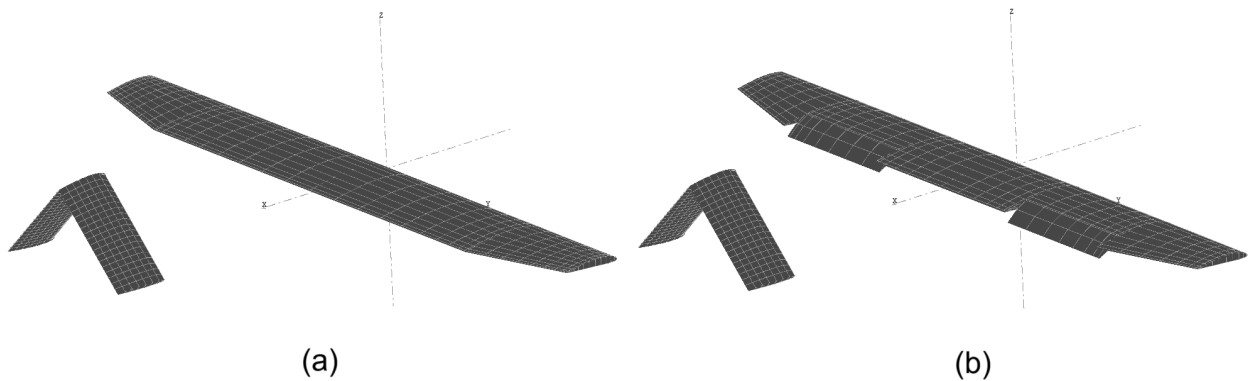
7

(a)   (b)

Figure 6 Carrier model: (a) Cruise (b) Flap deployed

IV.   Structural Design

Based on the carrier plane design parameters derived from research, trade studies, and simulations, the carrier CAD design was created. Autodesk Inventor was the primary CAD tool used to create the CAD model. As mentioned before, one of the main design principles of the carrier was to reduce weight. Thus, material selection was crucial for weight saving. Furthermore, as we will be conducting various test flights on the carrier, we expect the airframe to undergo substantial stress and damage. Thus, repairability was also a key factor.

The main structure of the plane was decided to be constructed using four carbon fiber tubes, similar to bird bones. Two carbon fiber tubes act as tail booms running along the length of the plane, with one for each fuselage. These carbon fiber tubes are connected using aluminium machined blocks to the two carbon fiber tubes acting as wing spars, as shown in Figure 8 (d). The bone structure is the core of the carrier, and all components will be attached to the bone structure, such as motors, electronics, batteries, and landing gear. Using carbon fiber tubes allows for easy replacement should one get damaged. The aerodynamic fairings of the fuselage will be formed by a fiberglass composite shell. This shell is intended to make the fuselage aerodynamic and protect the electrical components from particles and debris such as dust. Since the shell will not be used to support components, a thin two-layer fiberglass will be used to minimize weight. The CAD plan of the shell is shown in Figure 8 (a), and the fiberglass lay-up prototype results are shown in Figure 8 (c). The main wing and tail will be constructed from fiberglass-reinforced foam core. The reinforced foam core was selected over balsa coated with monokote due to the relatively low density and enhanced durability and repairability. Two airfoil-shaped wooden guides will be used to cut the foam core from the foam blocks using a hot-wire tracing the wood piece as a guide. The main wing will have two holes for attaching the carbon tube wing spars and a rectangular slot for routing servo connectors to the control surfaces. For the center section of the wing, the slot will be larger to accommodate power wire connections between the two fuselages.

There were two landing gear designs: fixed and retractable. At the point of submitting the abstract of this paper, a retractable design was adopted to further reduce drag during cruise flight. However, later research revealed that the retractable landing gear introduces more complexity than desired, such as additional servo and reinforced components. These changes add up to significant weight to the extent that the reduction in drag cannot compensate for the increase in weight. As a result, a simple fixed gear constructed from two machined aluminium plates was adopted. Furthermore, to minimize the vibration to the 8-10 lb airframe during taxiing, a spring suspension system was introduced. The gear is attached directly to the carbon fiber tail booms shown in Figure 8 (b).

Electrical components are highlighted in yellow in Figure 8 (b). The two 2200mAh 6s batteries will be attached below the fuselage carbon fiber tail boom. A 3d printed adapter with velcro straps will hold the battery in place. The carrier propulsion setup features two 4260 500kV motors with 11x11 inch propellers. Using this setup, the carrier aircraft is projected to have a thrust-to-weight ratio of 2.2, a top speed of 80mph in level flight, and a

maximum flight time of 9 minutes. Using this setup, the carrier aircraft would have a total of 97.5 Watt-Hours of stored energy and strong take-off performance due to the high thrust-to-weight ratio.
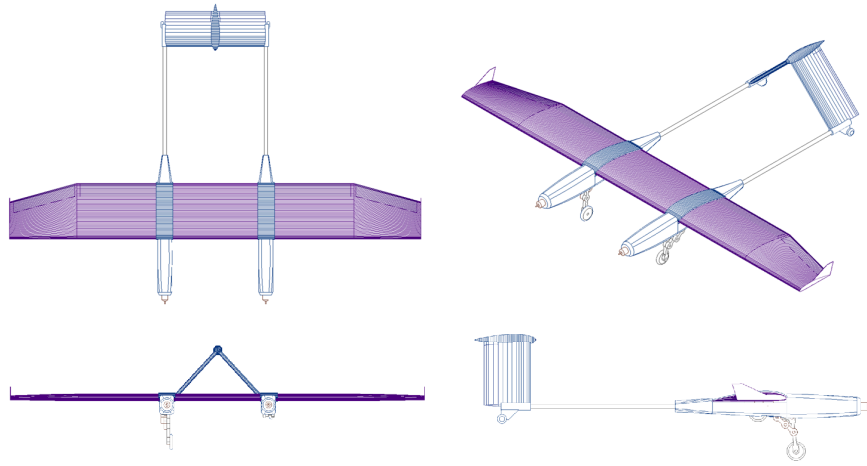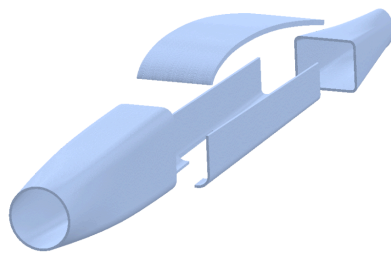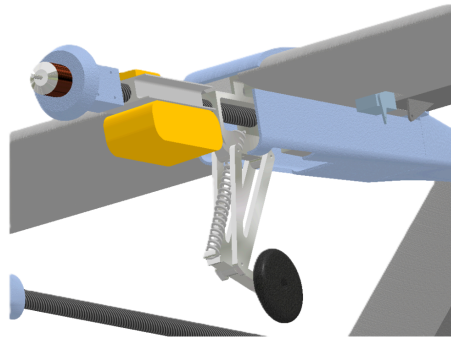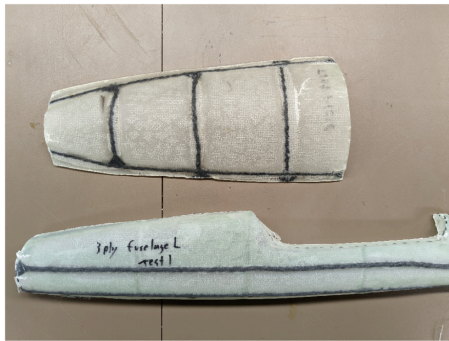

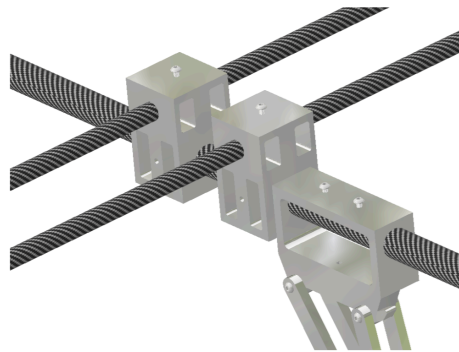**Figure 7 Carrier CAD design**

(a)

(b)

(c)

(d)

Figure 8 Carrier CAD and material testing: (a) Outer shell CAD (b) Carrier internal component placement CAD plan (c) Composite shell prototype (d) Carrier bone structure CAD

V.   Future Tasks, Prototyping, and Testing

The aerodynamic analysis and structural design of the carrier have been completed. The next step is to manufacture a prototype carrier and conduct flight testing to further refine the design of the carrier. Furthermore, the integration with the glider and the establishment of flight operation procedures must be done. There is knowledge to be gained from manufacturing the carrier that will influence future structural designs. Applicable to the carrier, aluminum machining tolerances or limitations of fiberglass lay-up geometries may cause the need to redesign some components. These know-hows are extremely variable and cannot be fully anticipated by research; thus, an experimental approach is crucial. As for flight tests and glider integration tests, determining the test procedures is necessary to ensure the safety of the team and prevent the loss of equipment. The flight test data will be recorded precisely and be used to improve the carrier design. In addition, the tested data could be compared to simulation data to explore the numerical and experimental error. Knowing the numerical study error will be useful in future projects undertaken by the team.

VI.   Conclusion

Carrier, a fixed-wing UAV capable of deploying an autonomous glider mid-flight for the 2025 AIAA DBF competition, was researched and developed. The development started from the sensitivity analysis of the point scoring system, revealing that a high cruise speed maximizes the resulting score. Based on the findings, the carrier plane design was created and refined using research, trade studies, and XFLR5 simulations. The carrier was designed to have a maximum velocity of 80 mph in level flight, a cruise velocity of 67.5 mph, and a minimum speed of 20.25 mph by utilizing deployable flaps. CAD designs were created based on the parameters resulting from the previous stages. The sturdy design and material were selected for their light weight and high repairability, considering the extensive flight tests in the future. We have created a solid baseline for the SPAROW project to proceed to the manufacturing and testing stages. The CAD and simulations verified the concepts and designs, thus minimizing design changes to be made after entering the manufacturing stage while keeping a relatively low cost. Furthermore, our team has accumulated a significant amount of knowledge and established a team structure capable of producing high-performance aircraft for future projects.

VII.   Acknowledgements

VIII.   References

[1]   Criollo, L., Mena-Arciniega, C., and Xing, S., "CLASSIFICATION, MILITARY APPLICATIONS, AND OPPORTUNITIES OF UNMANNED AERIAL VEHICLES," Aviation, Vol. 28, No. 2, 2024, pp. 115–127. https://doi.org/10.3846/aviation.2024.21672

[2]   Tsouros, D. C., Bibi, S., and Sarigiannidis, P. G., "A Review on UAV-Based Applications for Precision Agriculture," Information (Switzerland). 11. Volume 10. https://doi.org/10.3390/info10110349

[3]   Ackerman, E., and Koziol, M., "The Blood Is Here: Zipline's Medical Delivery Drones Are Changing the Game in Rwanda," IEEE Spectrum, Vol. 56, No. 5, 2019, pp. 24–31. https://doi.org/10.1109/MSPEC.2019.8701196